UNITED STATES DEPARTMENT OF THE INTERIOR

GEOLOGICAL SURVEY

A Cu-Ni-Mn-Zn mineral resource deposit model
for the northern Pacific Oceanic Basin

by

Joseph Moses Botbol[1]

U.S. Geological Survey Open File Report 90-402

1990

[1]United States Geological Survey
Branch of Atlantic Marine Geology
Woods Hole, MA 02543

CONTENTS

FIGURES

TABLES

Abstract

Cu, Ni, Mn, and Zn contents of manganese nodules in the north Pacific Oceanic Basin were analyzed to determine their relative contribution to a proposed model, which was later applied to the Clarion-Clipperton zone. Hypergeometric probability calculations showed that the spatial distributions of Cu, Ni, Mn, and Zn are not due to chance. Six areas in the northern Pacific are identified as being similar to the proposed model. Characteristic analysis, the method that was used, is effective at delineating favorable areas for future mineral resource exploration.

Introduction

Economic interest in deep ocean copper- and nickel-bearing manganese nodule research and exploration paralleled the decline in the price of nickel from the mid-1970's through the early 1980's (see Clark and Johnson, 1985). The high cost of deep ocean exploration was judged to be prohibitive under the circumstances of a declining market and an experimental mining and beneficiation process. In addition, only a very small percentage of the ocean bottom had been explored, and effective optimized ocean bottom exploration methods were just emerging. Consequently, many nodule research and exploration programs were curtailed, and the attentions of interested parties were turned to high cobalt content crusts occurring in shallow waters (<2000m.)

Free from the pressures of an active exploration environment, this lull in nodule interest has provided an opportunity to investigate the spatial distributions of deep sea manganese nodules. Furthermore, publicly available nodule data are comprehensive and, for the most part, static. This report deals with the analysis of data in a publicly available manganese nodule geochemical data-base that is well suited for the application of a recently developed multivariate analytical technique, characteristic analysis (McCammon, 1983).

Scope

This study is an extension of the work described in U.S. Geological Survey Bulletin 1863 (Botbol and Evenden, 1989). Original data consist of geochemical data describing approximately 1200 marine manganese nodule samples distributed throughout the northern Pacific Ocean. All data were processed on a COMPAQ 386/20 microcomputer operating under UNIX 3.0, with a math co-processor, and 100 Mbytes hard disc memory.

Data description

The manganese nodule sample data used in this report have a very low sample density (see fig. 1). Consequently, this study presupposes an assumption about the continuity of metal content distribution throughout the study area. This is reflected in the gridding process where selectable interpolation parameters are used to control the the area of influence and aggregated value at each grid intersection.

Data that are fixed in time and space were intentionally used in this study. The establishment of a fixed time frame of reference facilitates hypothesis testing involving data captured after the study. The data used in this study are summarized in detail in Botbol and Evenden (1989).

Data

Approximately 1200 samples from the Scripps Institute of Oceanography (SIO) nodule data bank (Frazer and Fisk, 1980) compose the data used in this study. The region of interest is bounded by 120°E., 100°W., 0°N., and 40°N. This region is further divided into 14 20° X 20° subregions. These are indicated by large 2-digit numbers in the upper and lower margins of the map in Figure 1, an index map of the studied area.

Depth of sample and geochemical analyses for Co, Ni, Mn, Fe, Cu, Zn, Pb, Al, and Si are the variables that constitute the unit record for the working data set. All variables are not necessarily measured at each sample site. Figure 1 shows the spatial distribution of sample sites for Ni, one of the variables with the highest sample frequency.

Gridding

A 28 X 77 grid of squares was superimposed over the study area, and geochemical data were interpolated using a 5 grid unit maximum search radius and an inverse squared-distance weighted least-squares function. After repeated trials of various combinations of grid unit sizes, search radii, and weighting functions, the above selected parameters were considered to offer the most reasonable balance of data smoothing, filling of open space, and minimum distortion of the original ungridded surface portraying each variable. In this report, each cell is centered at a grid intersection, and the extent of each cell is halfway to the next grid intersection above, below, and on either side of the cell.

Characteristic analysis

Characteristic analysis is a technique which computes the weight or degree to which selected ternary transformed variables contribute to the description of a given "type area" or model, and then, for the same variables, computes the similarity between any selected site and the model. Details of the characteristic analysis procedure have been published in McCammon, et al. (1983), and are beyond the scope and intent of this report. A brief summary of the procedure follows.

Ternary transforms

The characteristic analysis procedure requires input data to be in ternary form whereby a desirable datum is given the value 1, a datum of unknown value is 0 (zero), and an undesirable datum is given the value -1. Blanks are assigned to absent data. A principal assumption in this study is that all data are either desirable or undesirable and, therefore, are either 1, -1, or blank. The data are still classified as ternary except that there are no zeros. They are omitted because the characteristic analysis procedure effectively ignores 0's, and the information content of the already low sample density data set would be further diminished by their inclusion.

The criterion used here for ternary data assignment is the negative of the sign of the 2nd derivative of a 3 X 3 grid-unit window of the gridded data surface centering on each grid intersection and moving about the entire region. If the sign of the 2nd derivative is positive, the central datum is below the local regional inflection point, and is assigned a -1. If the sign is negative, the datum is above the inflection point, and is given the value 1. In other words, using this criterion all data lying above their local inflection points are local positive anomalies, and conversely. Data lying on an inflection point are arbitrarily considered positive anomalies and, therefore no point was assigned a 0.

The reader should take note that characteristic analysis is data amplitude independent. If any attribute at any model or regional site is considered favorable, regardless of the size of the original data value, the site is assigned a +1 for that variable.

Model construction and similarity scores

There are two basic parts to characteristic analysis; (1) to compute the degree to which each of a group of selected attributes defines a model, and (2) with respect to the selected attributes, to compute the degree of similarity between any selected site and the model.

In part 1 of the analysis, the union of attribute intersections in the area(s) designated as the model are used to compute the normalized weight for each variable. The first step in this part of the analysis is to compose a matrix called the product matrix. This matrix contains the numbers of intersections of all pairs of component variables and, in mathematical terms, is the product of multiplying the original ternary data matrix by its transpose. The first principal component of the product matrix yields the contribution of each of the variables. These contributions, or weights, are then normalized so that the sum of their squares equals 1.

In part 2 of the procedure, weights of the variables of the model are multiplied by the ternary values of corresponding variables at each site in the study area and aggregated to yield a similarity score. This is the final product of the analysis, and is usually portrayed on a map of similarity scores for all valid sample sites. If any model component attribute is absent from a regional site, no similarity score is computed.

Clarion-Clipperton model

The area with the highest manganese nodule abundance (Cronan, 1980; Clark, 1990), and the most dense sampling pattern in the entire northern Pacific study region is the Clarion-Clipperton zone located between the Clarion and Clipperton fault zones in subregions 7, 8, and 9. The model area is specifically identified in figure 1 and shown in all other figures as an area of contiguous individually outlined cells in the southeast of the study region. The western and eastern boundaries of the model area are the regions of the Line Islands and the Mathematicians Seamounts, respectively. Almost all samples were taken from depths between 3,000 and 5,500 m. A hypergeometric probability was used to test model components for significance, and after selecting the model variables, the model area was partitioned to test for robustness and internal consistency.

Selection of variables

After reviewing the spatial distributions of Co, Ni, Mn, Fe, Cu, Zn, Pb, Si, and Al contents in nodules (see figs. 2a, 3a, 4, 5a, 8 - 13), the Clarion-Clipperton zone was selected as the area for a model composed of Cu, Ni, Mn, and Zn. This selection was based on the fact that Cu, Ni, Mn, and Zn all have elevated concentrations in the zone, and the sampling density is the highest of the entire region. The high sample density and large area relative to the size of the study region also ensure model stability.

Ternary transformed data

Figures 2b, 3b, 4b, and 5b show the spatial distributions of the ternary transformed data. In subregions 07, 08, and 09 model variables are portrayed by a distinct checkerboard pattern coincidental with the Clarion-Clipperton zone. This pattern depicts gridded data values rapidly fluctuating about local inflection points.

The checkerboard pattern is possibly due to the high sample density of the model area causing a diminution of area covered by the geometry of the interpolation algorithm, thereby reflecting the aggregate of only those values very close to the local grid points. Another explanation for this pattern is that the area is enriched in the selected model components, and the enrichment is not uniform in the higher levels of concentration.

Since the ternary patterns of all selected variables are portrayed by the checkerboard pattern in the model area, this author feels that their mutual coincidence within the zone, as implicitly verified by hypergeometric probability (discussed later), has minimal affect on characteristic analysis model composition and utility. However, further detailed studies of this zone would most likely benefit from regridding and[or] the use of appropriate filters.

Except for the checkerboard pattern in the Clarion-Clipperton model area, the rest of the study area can be described as having isolated irregularly shaped islands of 1's, from 1 to 5 grid units across in the x and y directions, which are set in a regional matrix of -1's.

Hypergeometric probability

A hypergeometric probability function (McCammon, 1983, p. 81) was used to test the Clarion-Clipperton model for the likelihood of the spatial distribution of its components NOT being due to chance. High probabilities between variables indicate that the placement of the values of the variables in the model area is not random or not due to chance. If the model composition is not due to chance, obviously something must have caused the spatial distributions of the component variables to intersect as they do. The nature of this cause and effect is, however, not disclosed in the probabilities that are generated, and lies in the domain of geologic interpretation. Low probabilities indicate a model with a random distribution of data. Table 1 shows the probabilities for each of all pairs of variables that compose the Clarion-Clipperton model.

	Ni	Cu	Zn
Cu	1.00		
Zn	.97	1.00	
Mn	1.00	1.00	.74

TABLE 1. Probabilities of Clarion-Clipperton model variables being NOT due to chance.

As is shown in Table 1, the exceptionally high probabilities indicate that the Clarion-Clipperton model is certainly not a random model. Of the four component variables, zinc has lowest probabilities and is, therefore, the most randomly distributed. However, the Zn probabilities are sufficiently high that the degree of its randomness is most likely negligible.

Partitions of the Clarion-Clipperton model

To test the robustness of the composition and data distribution in the Clarion-Clipperton model, it was spatially divided into 4 separate partitions; the northern half, southern half, eastern half, and western half. Each partition was treated as a separate principal model and for each one hypergeometric probabilities were computed and are presented in Tables 2 through 5.

	Ni	Cu	Zn
Cu	1.00		
Zn	.76	.98	
Mn	1.00	1.00	.93

TABLE 2. Probabilities of variables in the northern partition being NOT due to chance.

	Ni	Cu	Zn
Cu	1.00		
Zn	.97	.94	
Mn	1.00	1.00	.31

TABLE 3. Probabilities of variables in the southern partition being NOT due to chance.

	Ni	Cu	Zn
Cu	1.00		
Zn	.18	.75	
Mn	1.00	.99	.24

TABLE 4. Probabilities of variables in the eastern partition being NOT due to chance.

	Ni	Cu	Zn
Cu	1.00		
Zn	1.00	1.00	
Mn	1.00	1.00	.93

TABLE 5. Probabilities of variables in the western partition being NOT due to chance.

In the 4 partitions of the Clarion-Clipperton model, Cu, Ni, and Mn show no less than a 0.99 probability of their spatial distributions being not due to chance. Zn, however, varies from a 0.18 with Ni in the eastern partition, to 1.00 in the western partition which has the highest overall probabilities of all components being not due to chance. The question that must be addressed here is whether or not the western partition should become the principal model area instead of the entire model area as originally defined.

To answer this question, one must consider two major attributes of the host region of the original model; (1) relative consistency of depth as compared with the western part of the entire study area (see fig. 13) and, (2) no perceivable major geochemical disruptions or changes throughout the zone when considered at the small scale of this study (see figs. 2a, 3a, 4a, 5a). Therefore, the advantages of the robustness of the larger sample population of the entire original model are preferred to the considerably smaller population but very slightly higher distribution probabilities associated with the variables of the western partition. Therefore, the whole of the Clarion-Clipperton model area is the model selected for this study.

Weights of variables

The following table presents the characteristic analysis model component weights computed for Cu, Ni, Mn, and Zn for the entire Clarion-Clipperton model area as well as those for each of the four partitions.

		Partition			
Variable	Whole model	North	South	East	West
Cu	.570	.556	.584	.577	.561
Ni	.564	.545	.584	.576	.561
Mn	.481	.519	.433	.515	.465
Zn	.354	.353	.363	.263	.394

TABLE 6. Weights of variables in the Clarion-Clipperton model and partitions.

The salient feature of Table 6 is that excepting identical weights of Cu and Ni in the south and west partitions, the decreasing ranks of the variables is consistently in the order Cu, Ni, Mn, and Zn. Zn is distinctively the lowest weighted variable of the model and all its partitions.

Northern Pacific regional analysis

Similarity scores were computed for 967 non-model (i.e., regional) cells, and 155 model cells in the study area. Only those points having all selected variables were considered, and a frequency distribution of the similarity scores is shown in Table 7.

Class	Score Interval		Model Cells		Non-model Cells	
			Freq	Pct	Freq	Pct
1	-1.000	-0.900	60	38.710	559	57.808
2	-0.900	-0.800	0	0.000	0	0.000
3	-0.800	-0.700	0	0.000	0	0.000
4	-0.700	-0.600	12	7.742	50	5.171
5	-0.600	-0.500	13	8.387	73	7.549
6	-0.500	-0.400	9	5.806	72	7.446
7	-0.400	-0.300	0	0.000	0	0.000
8	-0.300	-0.200	0	0.000	0	0.000
9	-0.200	-0.100	3	1.935	14	1.448
10	-0.100	0.000	4	2.581	16	1.655
11	0.000	0.100	11	7.097	31	3.206
12	0.100	0.200	5	3.226	39	4.033
13	0.200	0.300	0	0.000	0	0.000
14	0.300	0.400	0	0.000	0	0.000
15	0.400	0.500	1	0.645	12	1.241
16	0.500	0.600	5	3.226	28	2.896
17	0.600	0.700	19	12.258	43	4.447
18	0.700	0.800	0	0.000	0	0.000
19	0.800	0.900	0	0.000	0	0.000
20	0.900	1.000	13	8.387	30	3.102
		totals	155		967	

TABLE 7. Frequency distribution of similarity scores for the Clarion-Clipperton model in the northern Pacific.

Table 7 shows that the attributes of 57.8% of the non-model cells are quite distinctly dissimilar to, and the attributes of 3.1% of the cells are quite distinctly similar to, those of the model. Figures 6 and 7 are grey-level maps of the distributions of similarity scores. The grey-levels in Figure 6 were selected on the basis of major breaks in the full range of the frequency distribution of similarity scores (table 7), and show both positive and negative similarities. The scaling of grey levels in Figure 7 eliminates low score clutter and distinguishes only the highest scoring areas.

There are 14 notably high similarity scoring areas in the entire study region, and these are located in subregions 02, 04, 05, 06, 08, 09, 10, and 13. Another slightly lower scoring anomaly is located in subregion 03. Six of the anomalies occupy single cells which, because of their lack of areal extent and their proximity to the model suggest that their significance be interpreted with caution, particularly in the absence of further larger scale analysis. The other anomalies occupy two or more cells and, for purposes of this analysis, it is assumed that the larger their individual included areas, the greater their significance. The largest of these (5 or more cells) are in regions 02, 04, 05, 10, and 13.

Anomalies occurring within in the model area show the distribution of similarity scores of parts of the model to itself. Because these cells were used in the computation of the weights, their significance has not yet been fully established.

Conclusions

Characteristic analysis to date has been untried in marine mineral resource applications. When applied to the SIO nodule data-base, characteristic analysis resulted in the generation of a Cu-Ni-Mn-Zn model in the Clarion-Clipperton zone which identified 14 areas that are highly similar to the model. These areas are consistent with the "deep occurrence" aspect of nodules, and all occur in relatively flat regions bounded by major structural and[or] topographic features (see Chase, 1971). Clark (1990) aptly refers to

these areas as "collecting basins".

The average median of each component variable of the model is higher than the median grade for those components in subregions with anomalies that are 5 cells or more (see Botbol and Evenden, 1989). However, the sample density in these subregions is also quite low, particularly considering the exceptionally small scale of the study. One cannot discount therefore the resource potential of the highly similar areas on the basis of the present metal content of the host subregions.

Characteristic analysis provides a rationale for further pursuit of details necessary to upgrade or discontinue efforts in the selected target areas. Additional efforts in the region would be valuable either for updating the existing data-base or using the newly acquired data for revising existing models for the occurrence of Cu-Ni-Mn-Zn mineral deposits.

References

1. Botbol, J.M. and Evenden, G.I., 1989, Descriptive statistics and spatial distributions of geochemical variables associated with manganese oxide-rich phases in the northern Pacific: U.S. Geological Survey Bulletin 1863, 62p.
2. Chase, T.E., Menard, H.W., and Mammericks, J., 1971, Topography of the north Pacific: Geologic Data Center, Scripps Institute of Oceanography, La Jolla, California.
3. Clark, A.L., 1990, Personal communication.
4. Cronan, D.S., 1980, Underwater minerals: Academic Press, London, 362p.
5. Johnson, C.J. and Clark, A.L., 1985, Potential of Pacific Ocean nodule crust, and sulphide mineral deposits: National Resources Forum, vol. 9, no. 3, United Nations, New York, p. 179-186.
6. McCammon, R.B., Botbol, J.M., Sinding-Larsen, R., and Bowen, R.W., 1983, Characteristic analysis - 1981: final program and a possible discovery: Mathematical Geology, Vol. 15, No. 1, pp. 59-83.
7. McKelvey, V.E., Wright, N.A., Bowen, R.W., 1983, Analysis of the world distribution of metal-rich subsea manganese nodules: U.S. Geological Survey Circular 886, 55p.
8. Frazer, J.Z., and Fisk, M.B., 1980, Availability of copper, nickel, cobalt, and manganese from ocean ferromanganese nodules (III): La Jolla, Calif., Scripps Institution of Oceanography, SIO reference 80-16 (prepared for U.S. Bureau of Mines), 117p.

Appendix

This appendix contains maps of the distributions of variables not included in the foregoing characteristic analysis, but that compose the original data-base from which the Cu, Ni, Mn, and Zn components were selected. These maps are as follows:

1. Figure 8. Distribution of cobalt content (%).
2. Figure 9. Distribution of iron content (%).
3. Figure 10. Distribution of lead content (%).
4. Figure 11. Distribution of aluminum content (%).
5. Figure 12. Distribution of silicon content (%).
6. Figure 13. Distribution of depth of sample (kilometers).

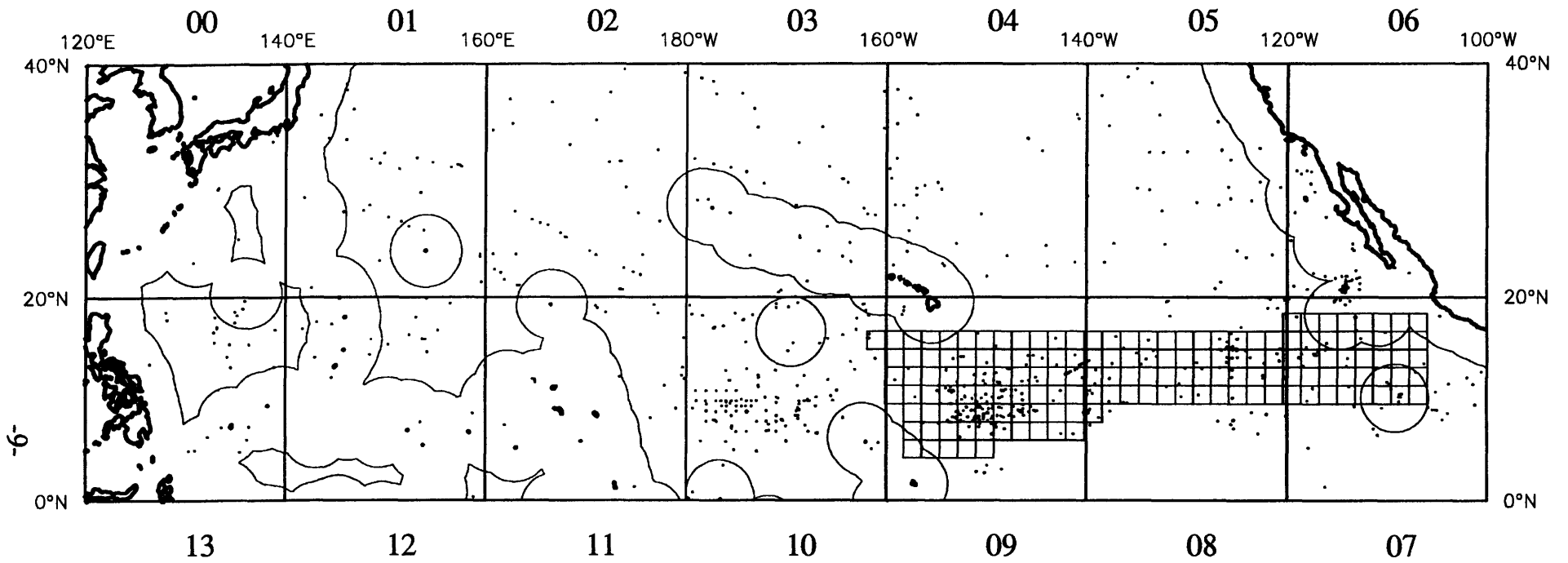

Figure 1. Index map of the northern Pacific study area showing continental boundaries (heavy lines), 200 mile limit (thin lines), Clarion-Clipperton model area (cell outline aggregate), subregions (indicated by large 2-digit numbers), and sample sites (small dots).

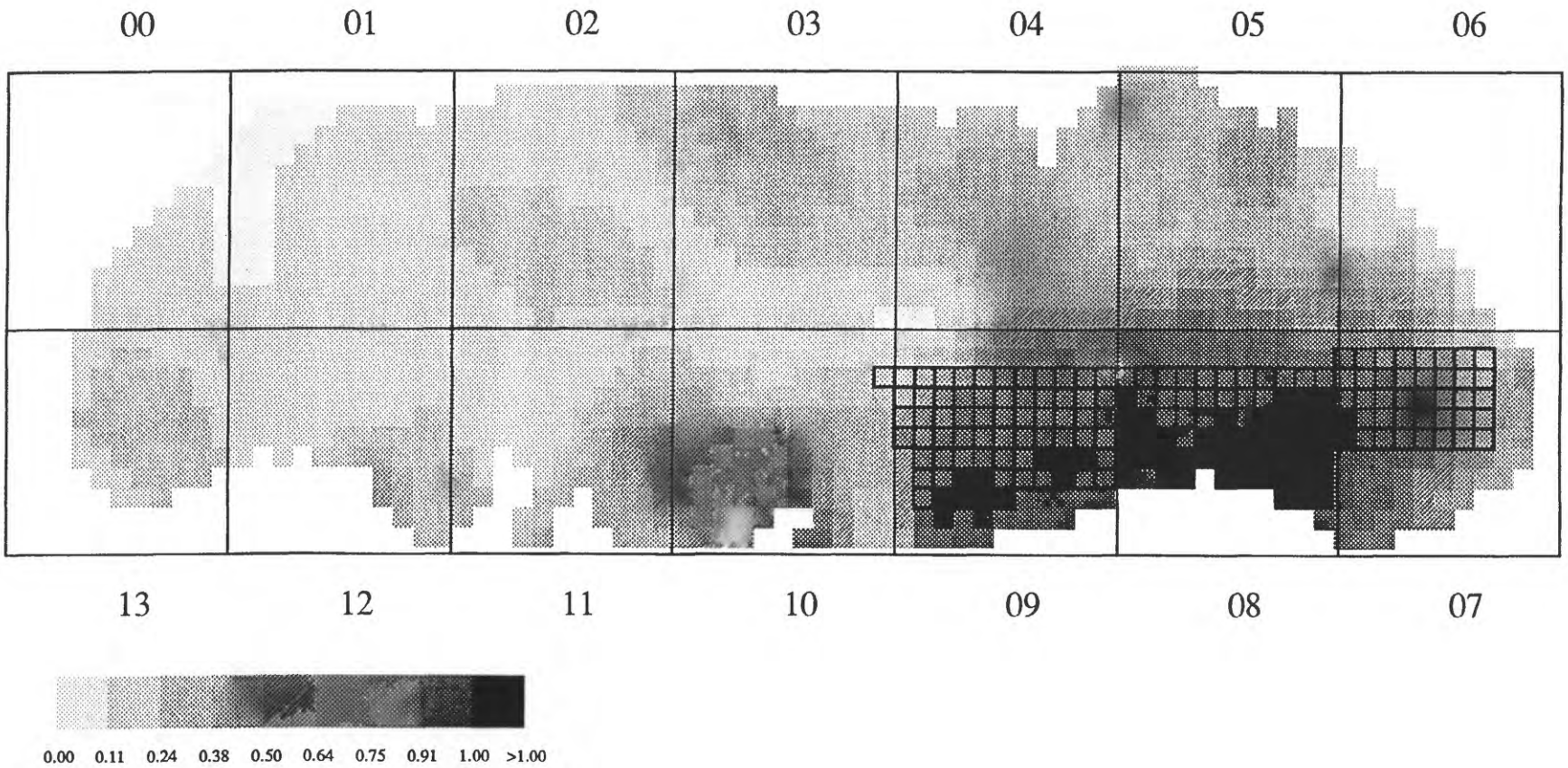

Figure 2a. Distribution of copper content (%) in the northern Pacific study area.
Cells outlined in black compose the Clarion-Clipperton model area.

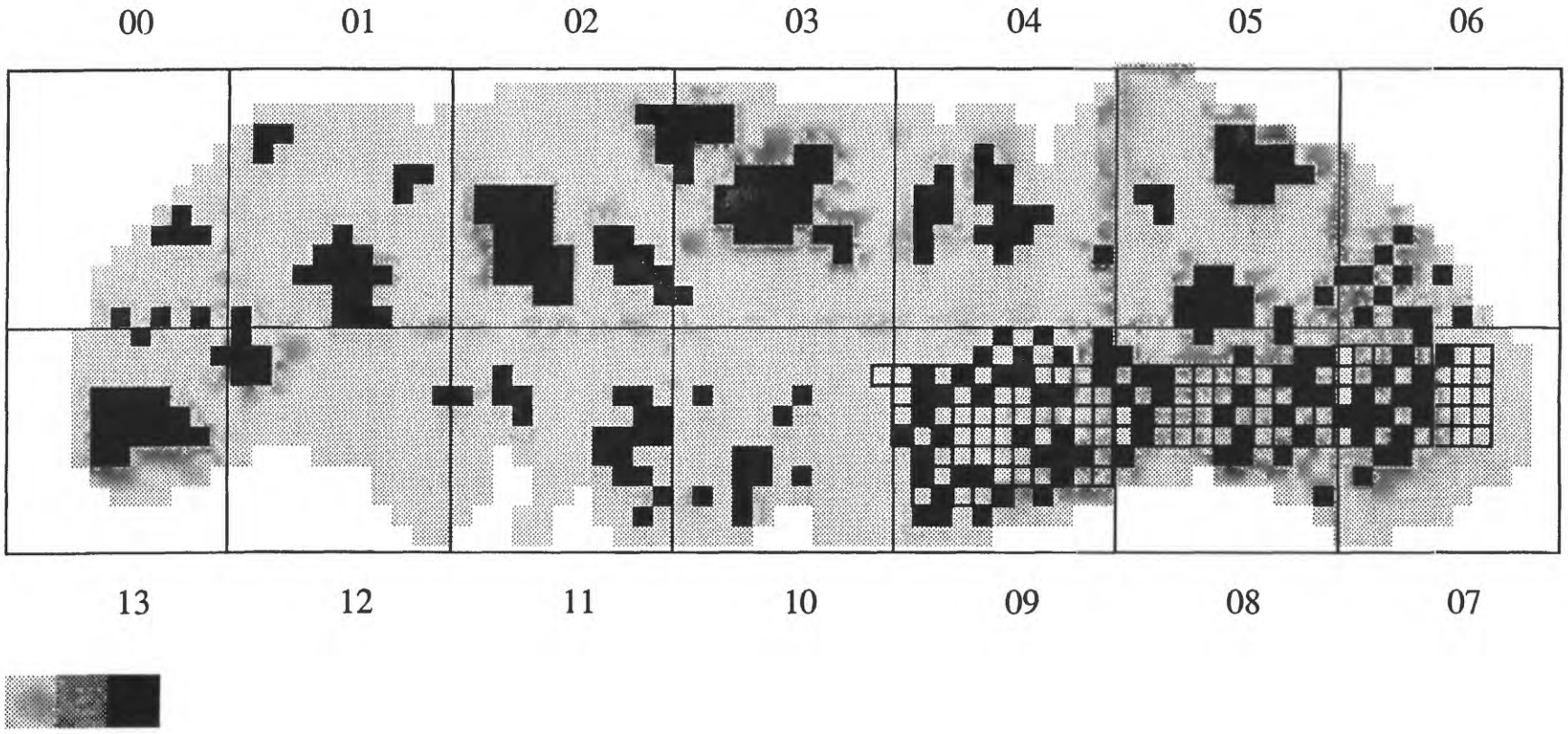

Figure 2b. Distribution of ternary transformed copper in the northern Pacific study area.
Cells outlined in black compose the Clarion-Clipperton model area.

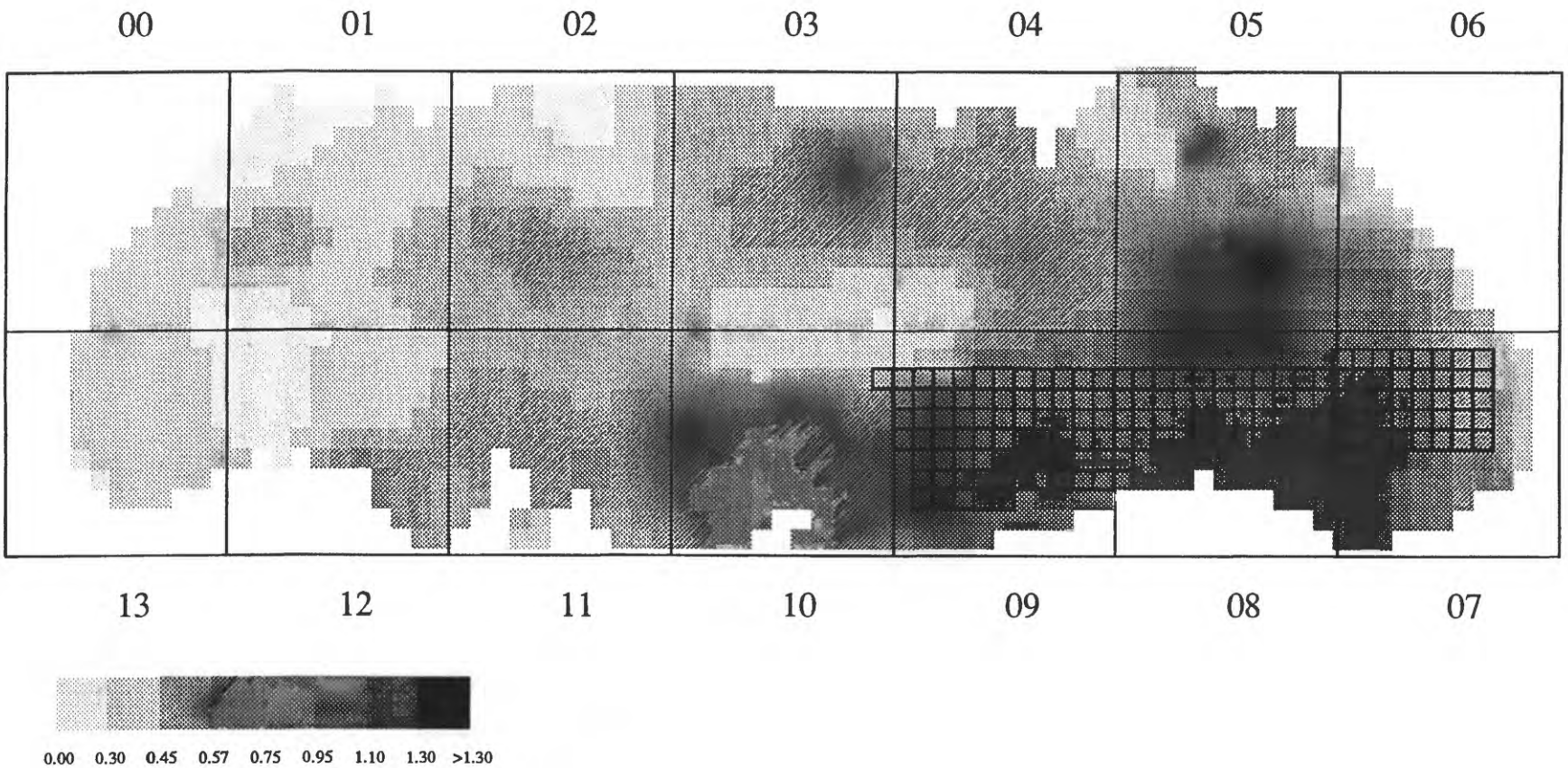

Figure 3a. Distribution of nickel content (%) in the northern Pacific study area.
Cells outlined in black compose the Clarion-Clipperton model area.

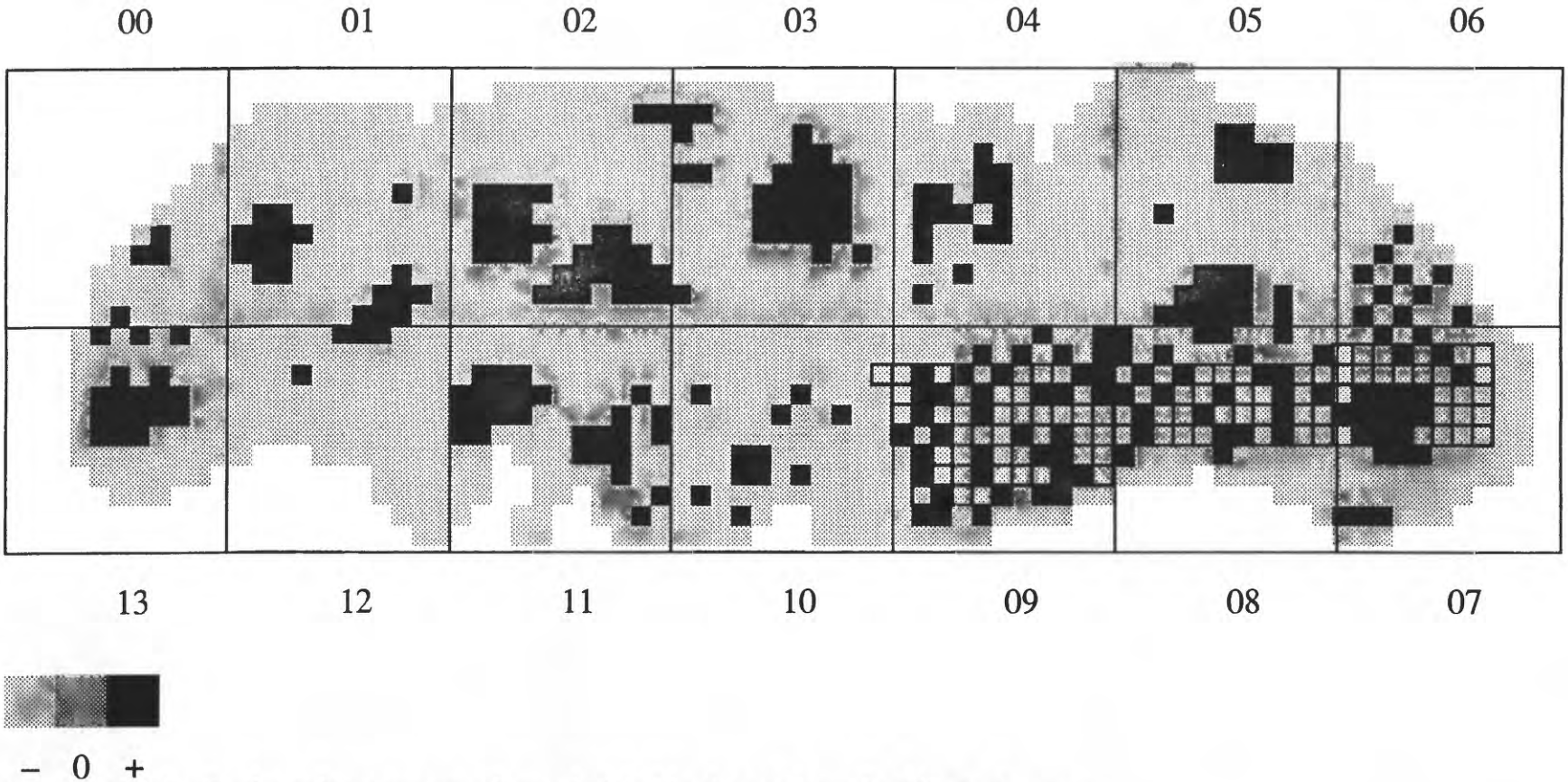

Figure 3b. Distribution of ternary transformed nickel in the northern Pacific study area.
Cells outlined in black compose the Clarion-Clipperton model area.

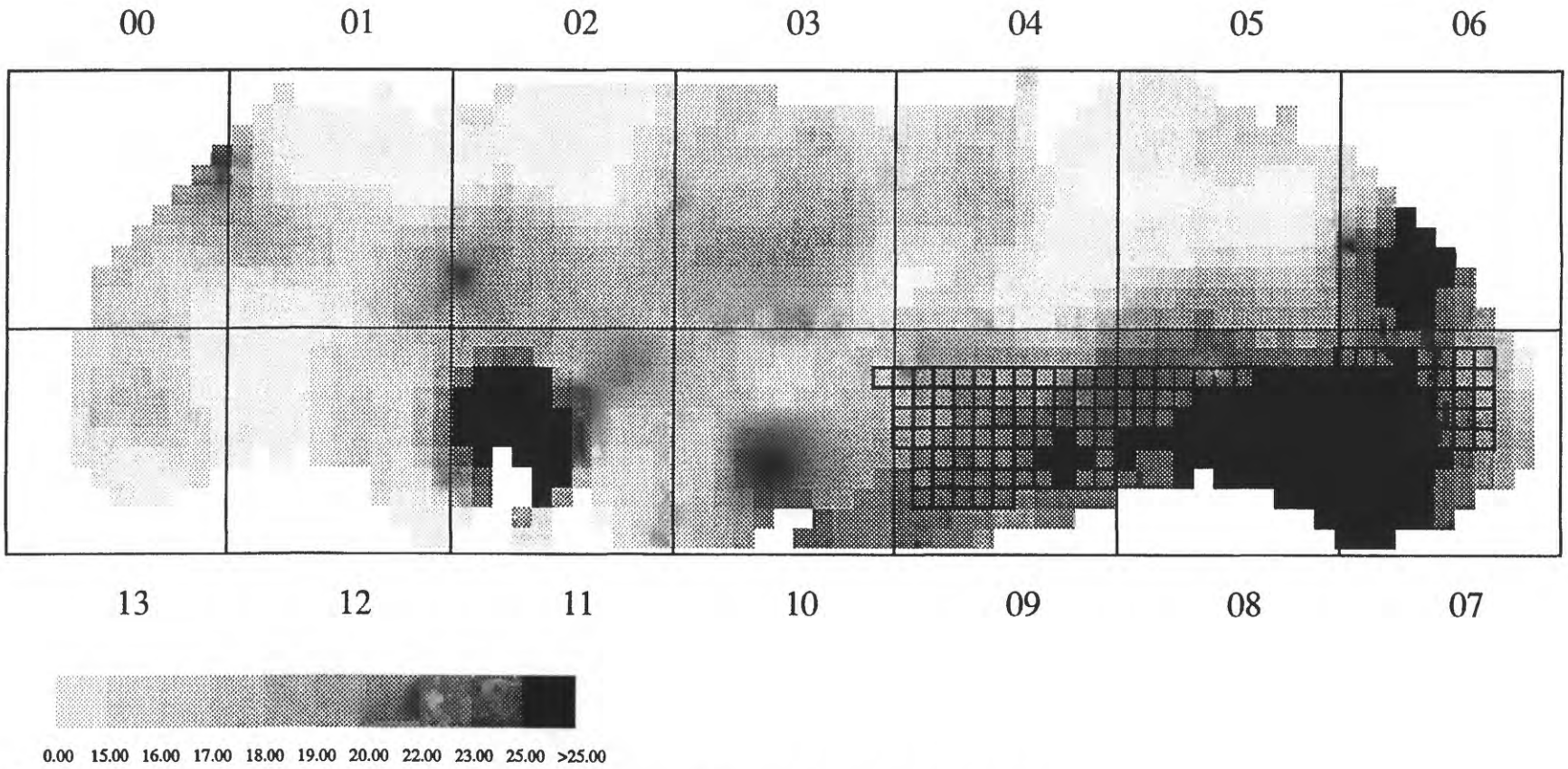

Figure 4a. Distribution of manganese content (%) in the northern Pacific study area.
Cells outlined in black compose the Clarion-Clipperton model area.

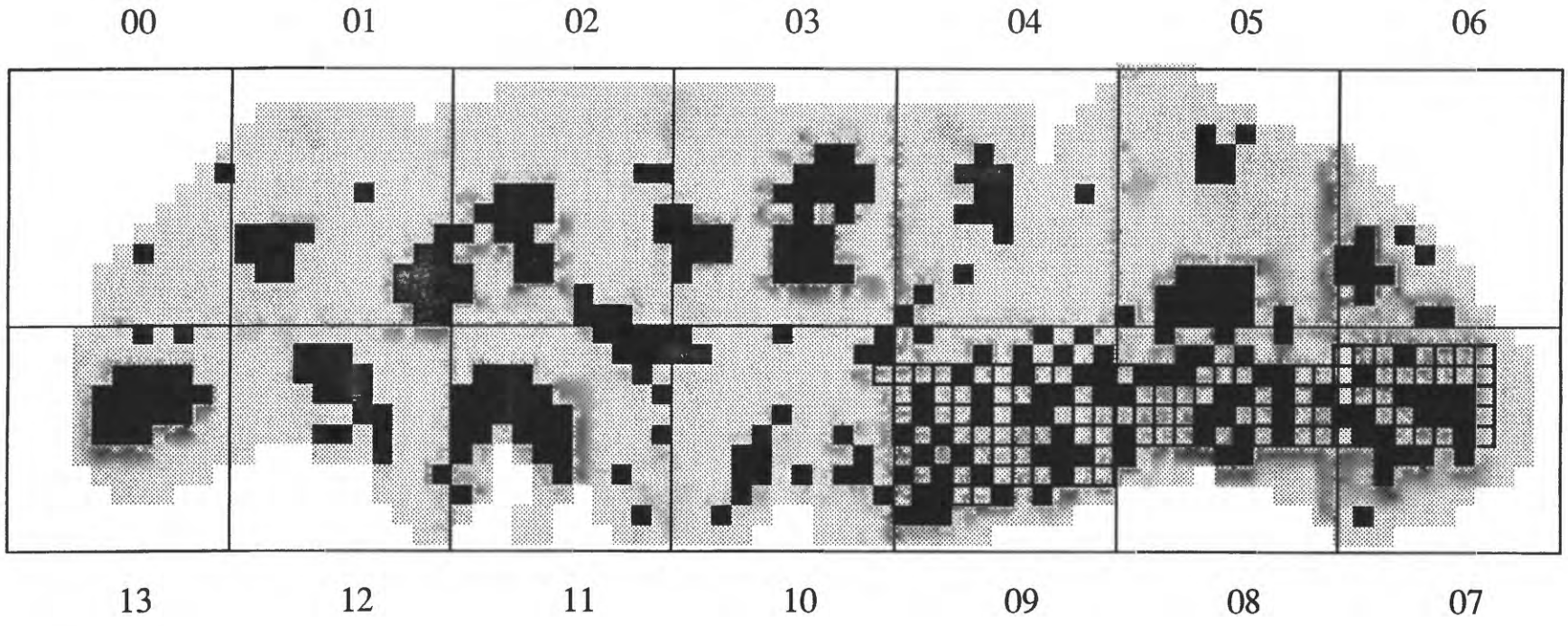

Figure 4b. Distribution of ternary transformed manganese in the northern Pacific study area.
Cells outlined in black compose the Clarion-Clipperton model area.

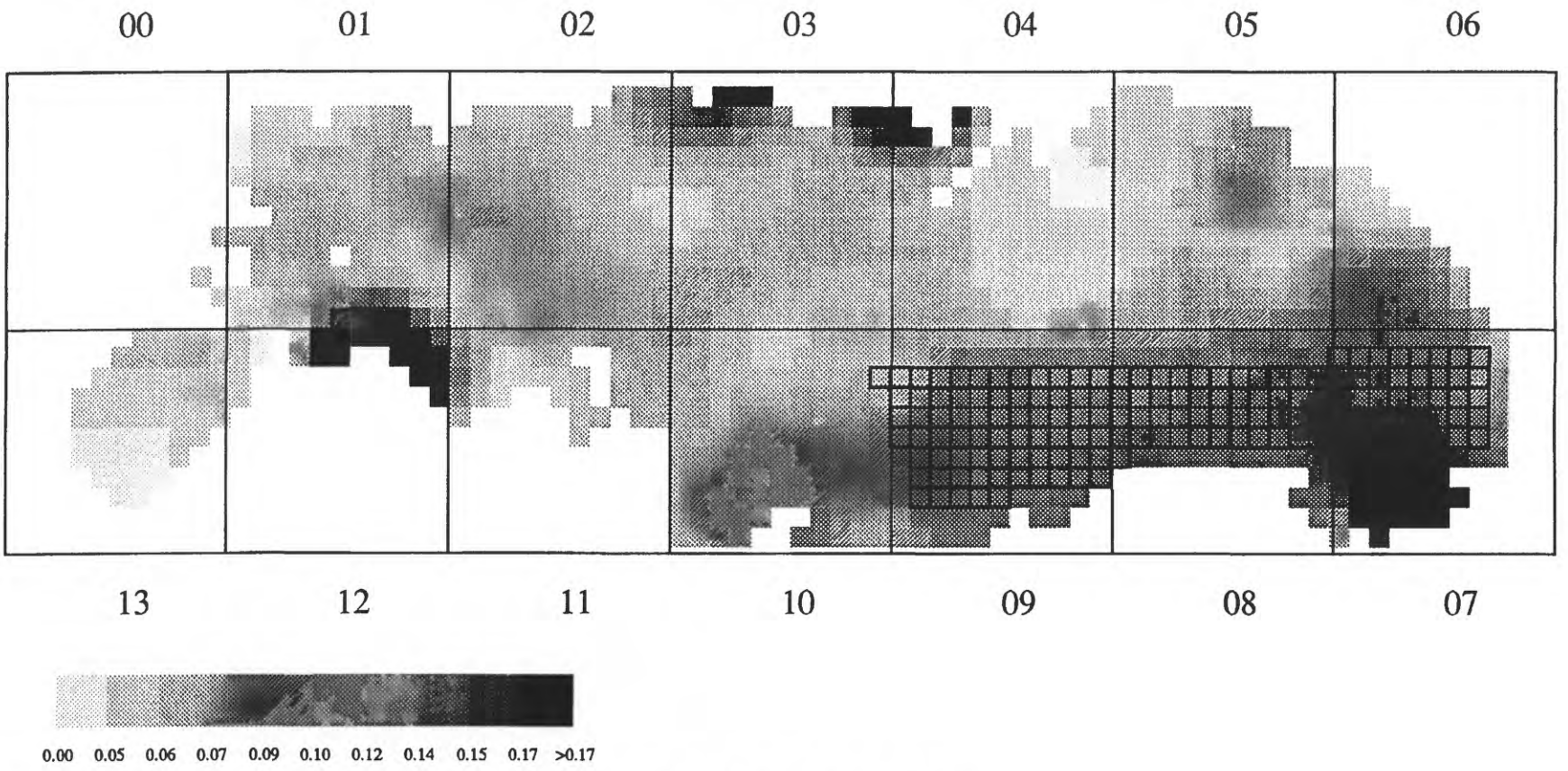

Figure 5a. Distribution of zinc content (%) in the northern Pacific study area.
Cells outlined in black compose the Clarion-Clipperton model area.

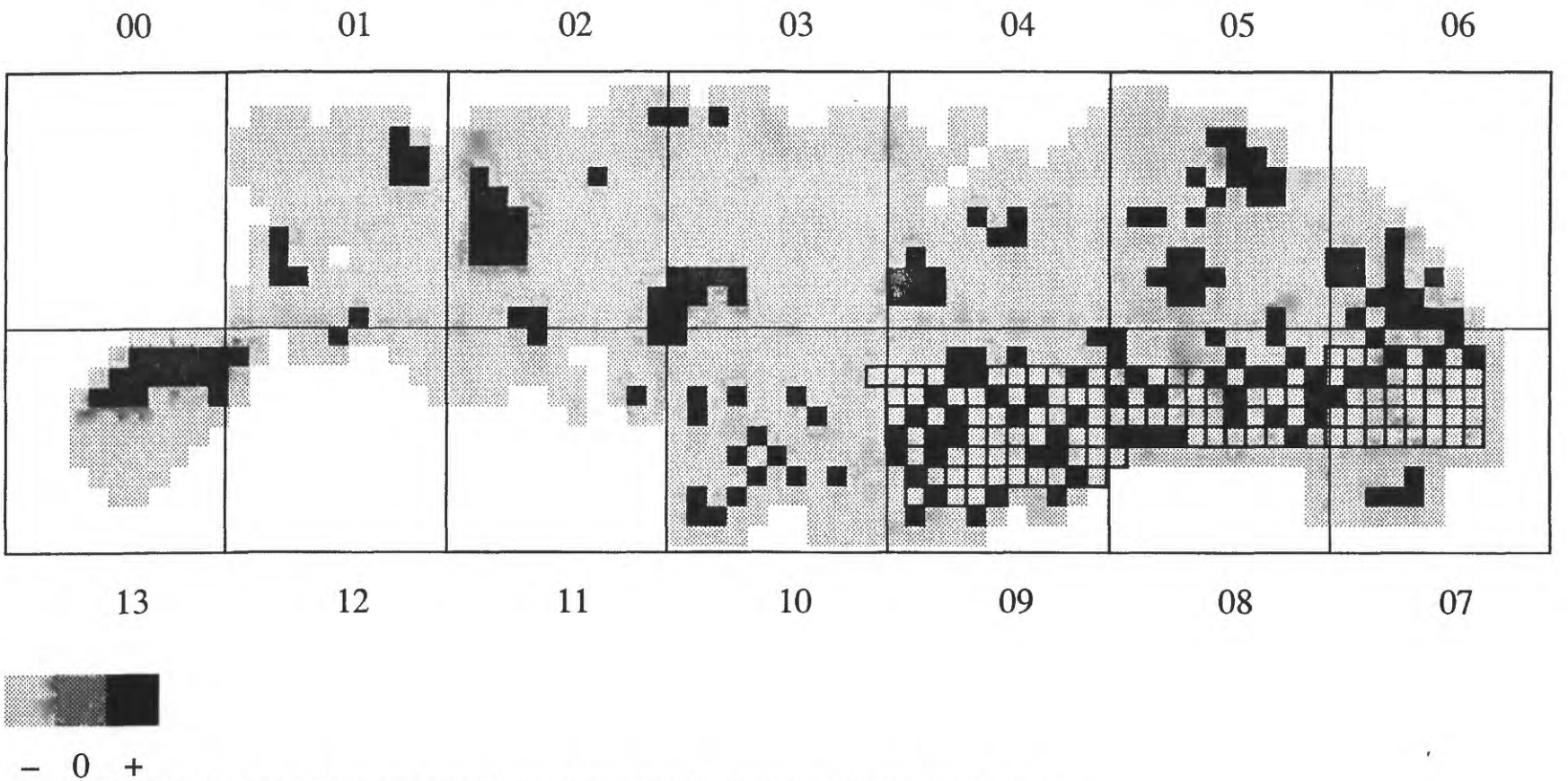

Figure 5b. Distribution of ternary transformed zinc in the northern Pacific study area.
Cells outlined in black compose the Clarion-Clipperton model area.

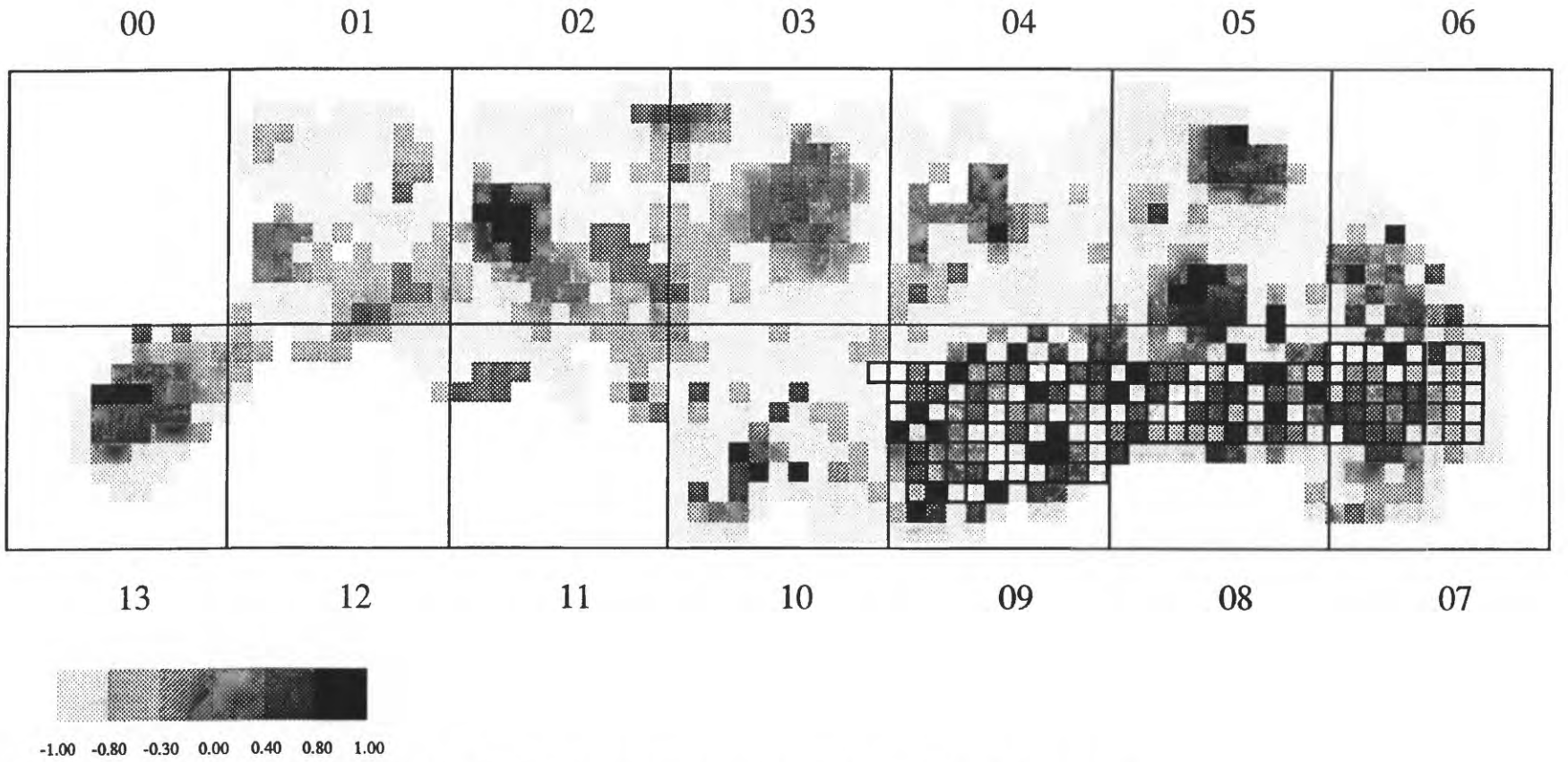

Figure 6. Distribution of Ni-Cu-Mn-Zn similarity scores in the northern Pacific study area.
Cells outlined in black compose the Clarion-Clipperton model area.

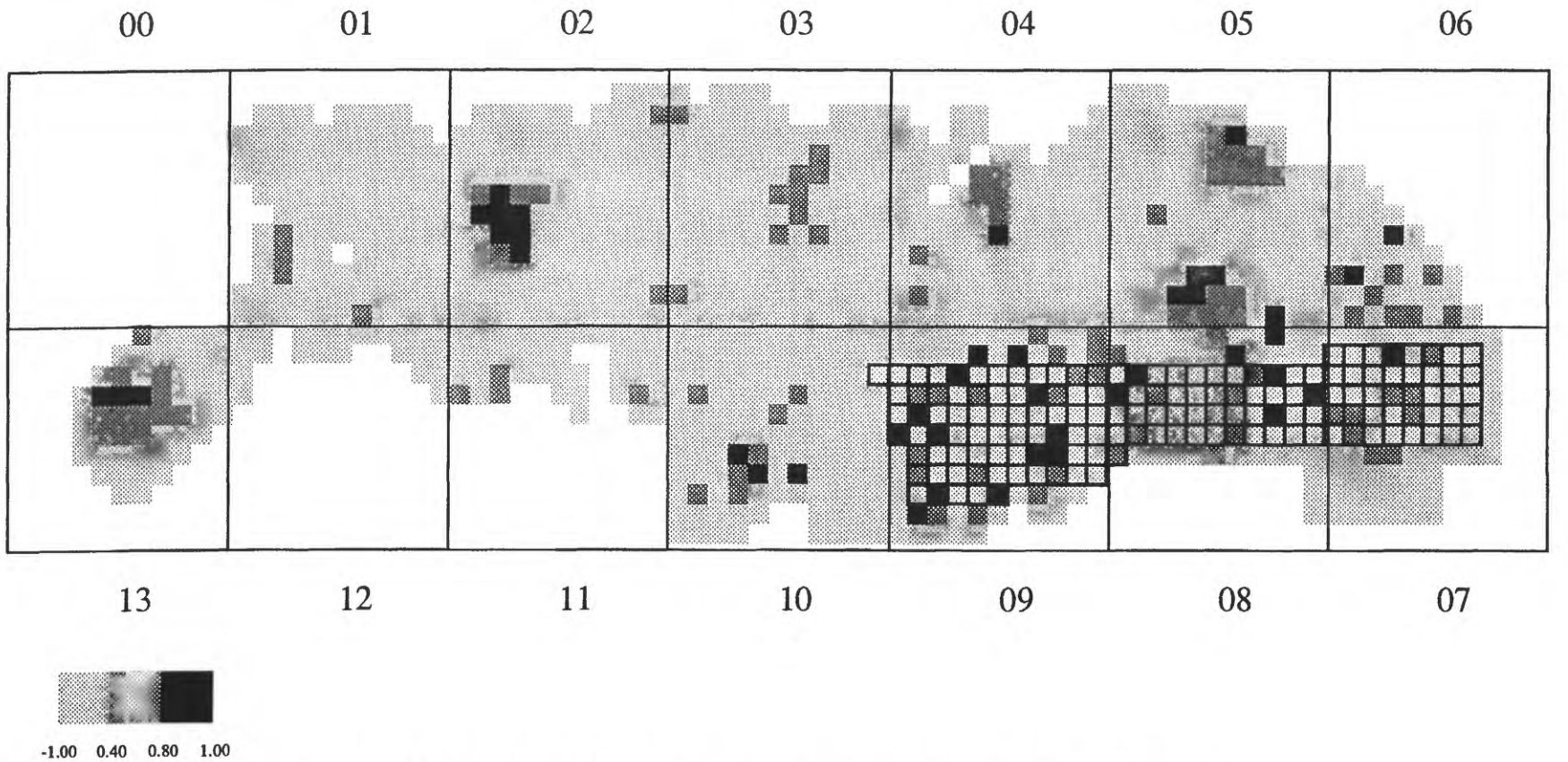

Figure 7. Distribution of highest Ni-Cu-Mn-Zn similarity scores in the northern Pacific Study area.
Cells outlined in black compose the Clarion-Clipperton model area.

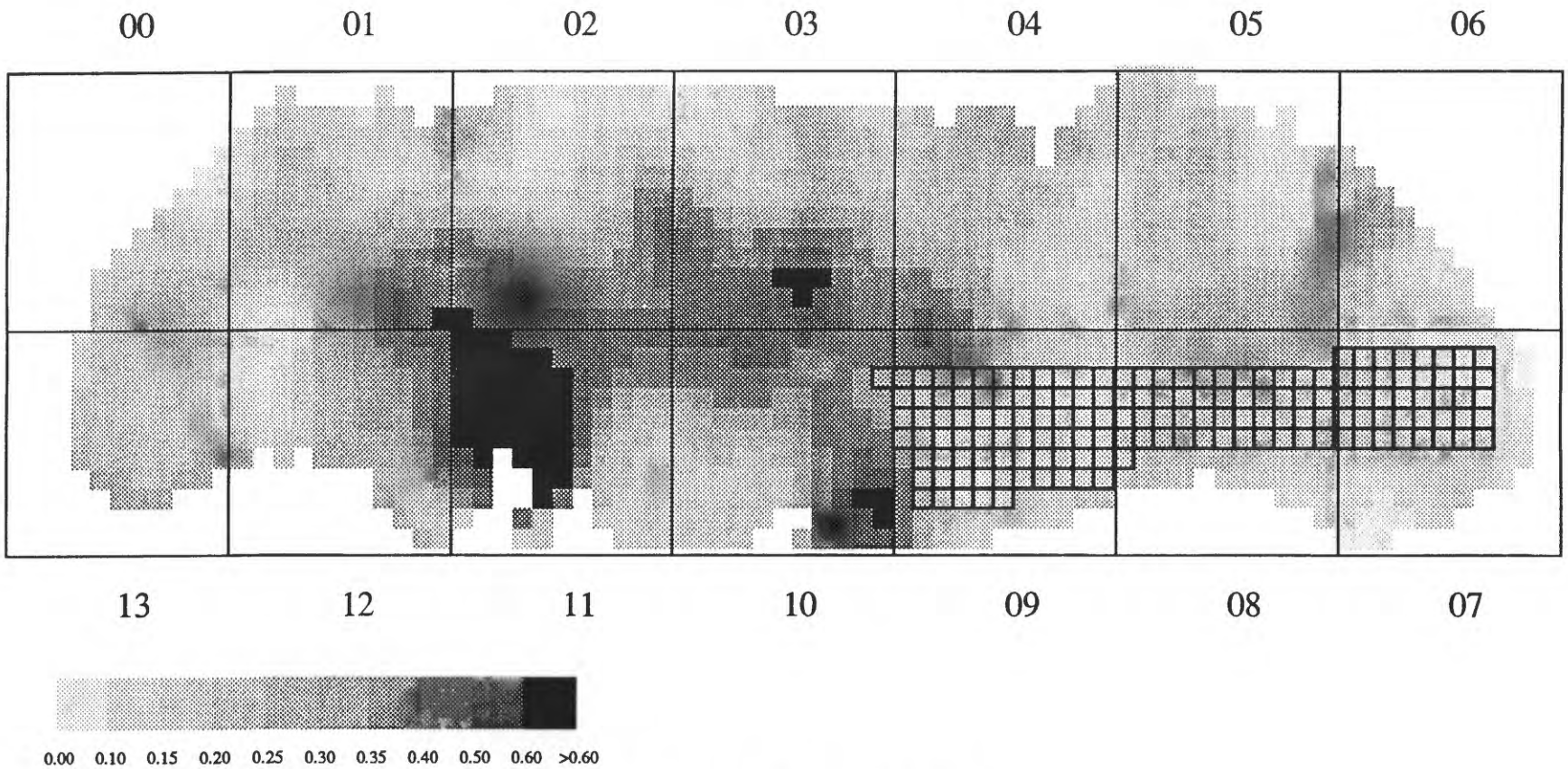

Figure 8. Distribution of cobalt content (%) in the northern Pacific study area.
Cells outlined in black compose the Clarion-Clipperton model area.

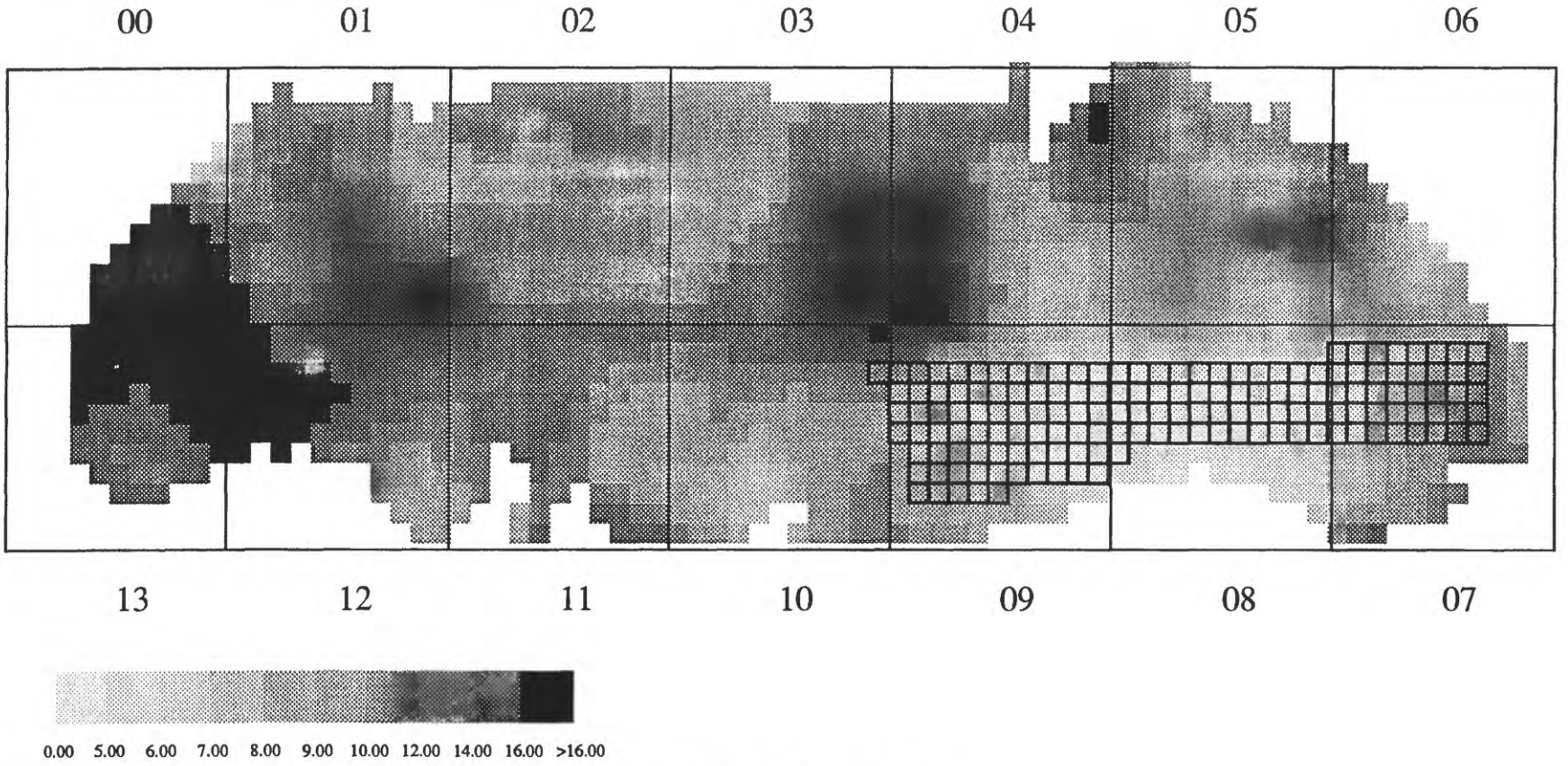

Figure 9. Distribution of iron content (%) in the northern Pacific study area.
Cells outlined in black compose the Clarion-Clipperton model area.

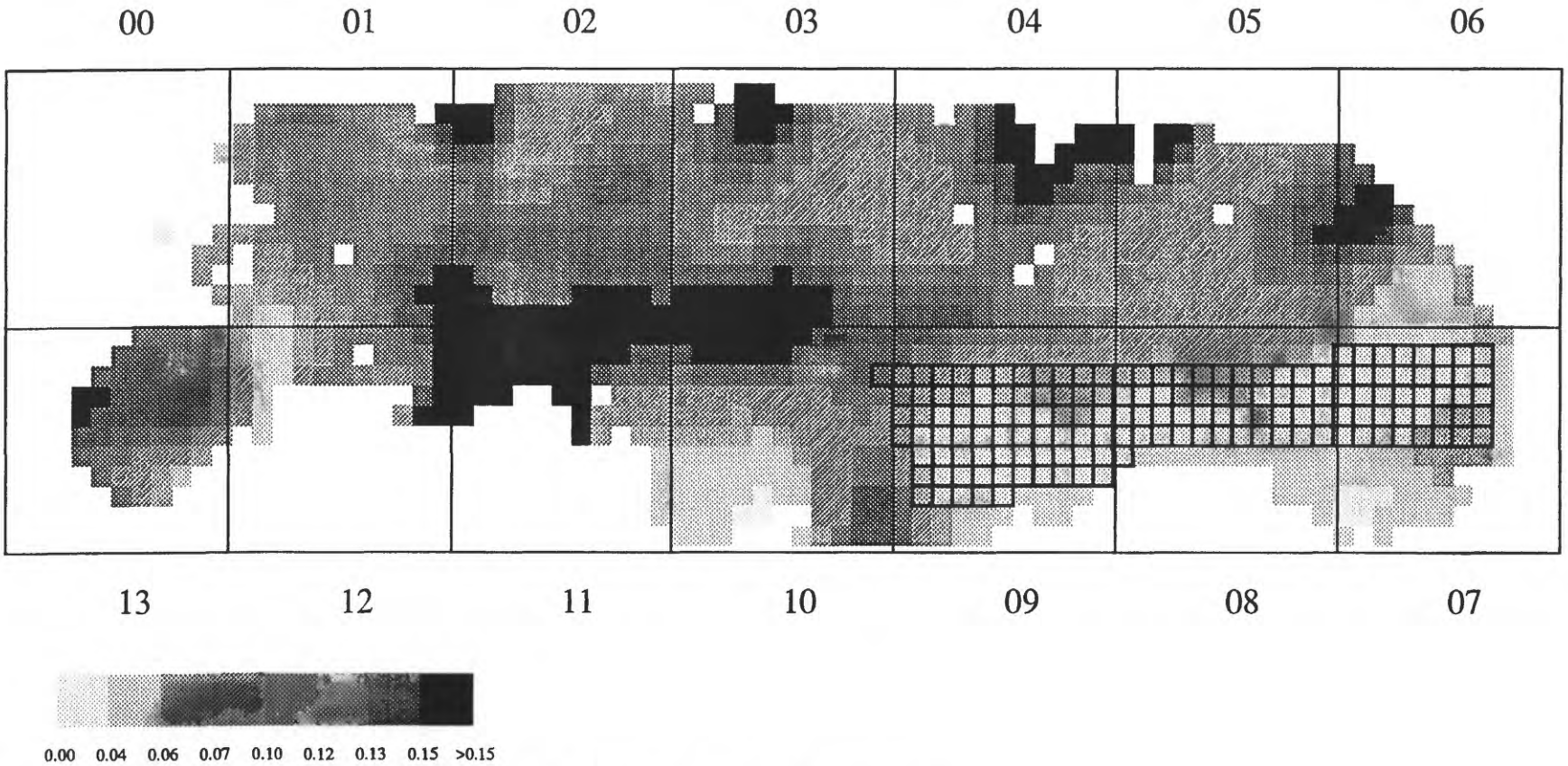

Figure 10. Distribution of lead content (%) in the northern Pacific study area.
Cells outlined in black compose the Clarion-Clipperton model area.

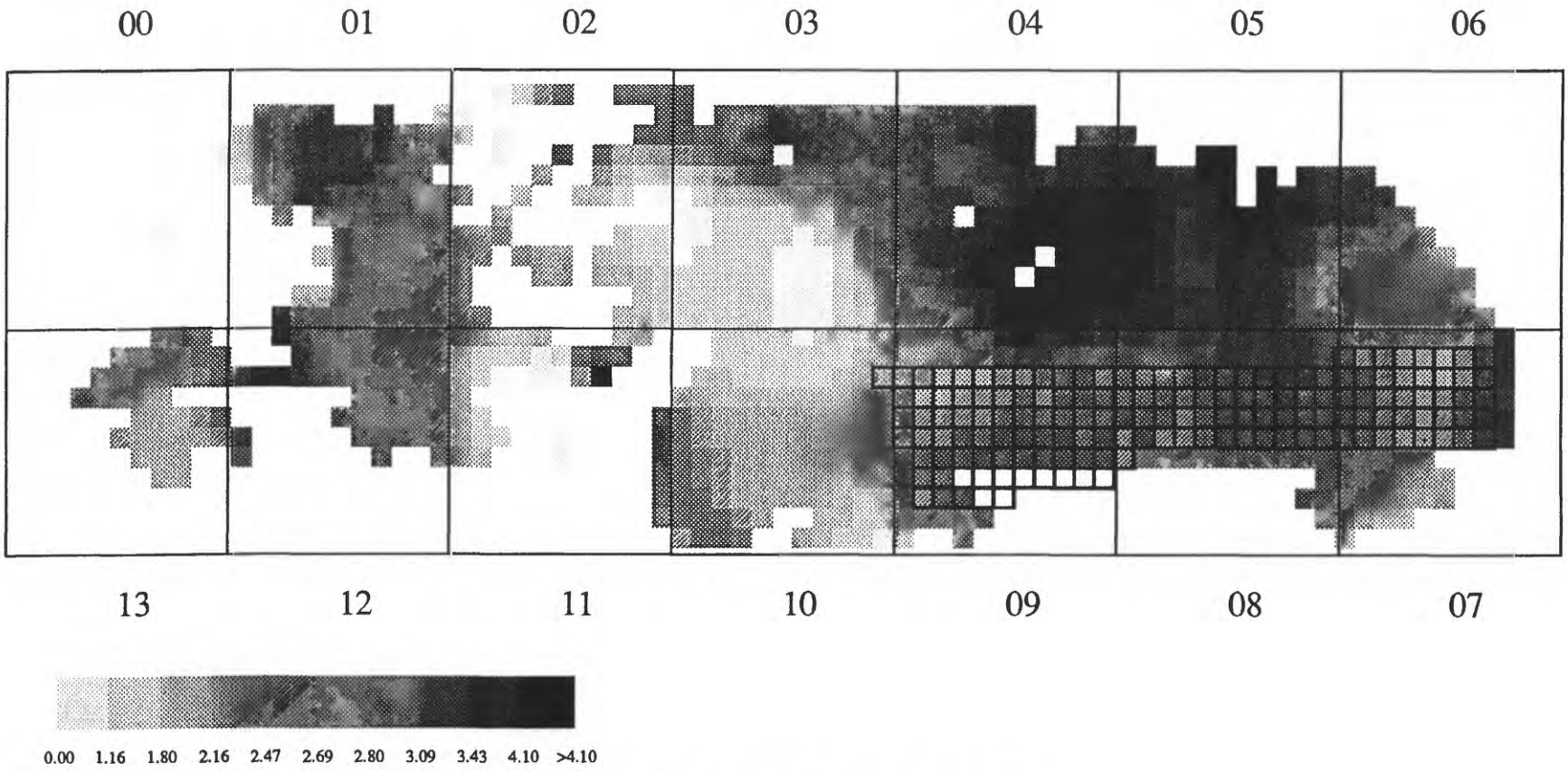

Figure 11. Distribution of aluminum content (%) in the northern Pacific study area.
Cells outlined in black compose the Clarion-Clipperton model area.

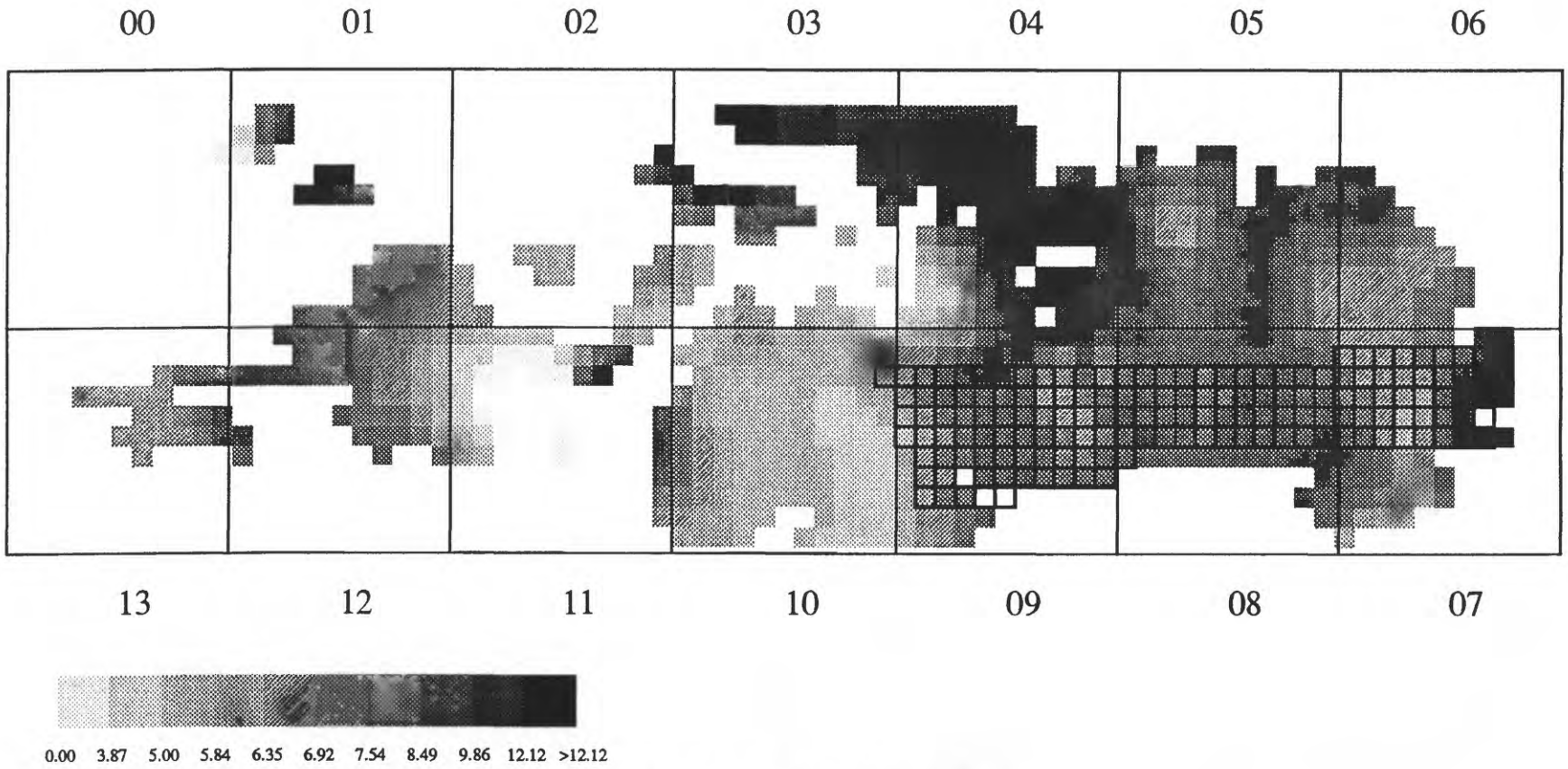

Figure 12. Distribution of silicon content (%) in the northern Pacific study area.
Cells outlined in black compose the Clarion-Clipperton model area.

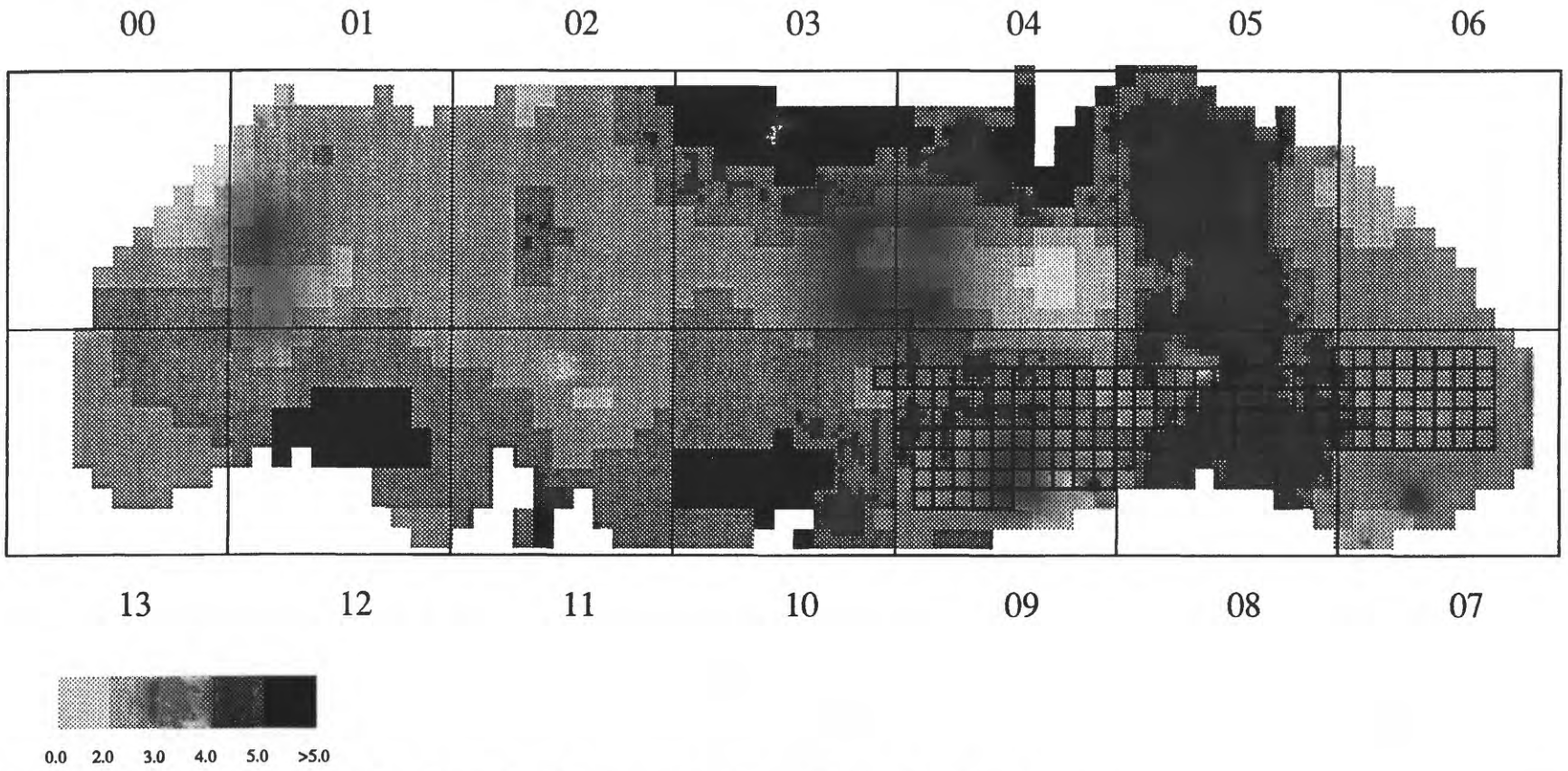

Figure 13. Distribution of depth of sample (kilometers) in the northern Pacific study area.
Cells outlined in black compose the Clarion-Clipperton model area.